



# The Open Construction and Building Technology Journal

Content list available at: [www.benthamopen.com/TOBCTJ/](http://www.benthamopen.com/TOBCTJ/)

DOI: 10.2174/1874836801610010136



## Structural Health Monitoring of Bridges Via Energy Harvesting Sensor Nodes

N. Bonessio<sup>1</sup>, P. Zappi<sup>2</sup>, G. Benzoni<sup>1</sup>, T. Simunic Rosing<sup>2</sup> and G. Lomiento<sup>3,\*</sup>

<sup>1</sup> Department of Structural Engineering, University of California at San Diego, La Jolla, California, USA

<sup>2</sup> Computer Science Department, University of California at San Diego, La Jolla, California, USA

<sup>3</sup> Department of Civil Engineering, California State Polytechnic University, Pomona, USA

**Abstract:** This paper deals with the application of novel sensing technologies to an existing Structural Health Monitoring (SHM) system for bridges. A vibration based SHM algorithm already in use to detect the structural performance degradation of a suspension highway bridge is modified to investigate the feasibility of replacing traditional wired accelerometers with state of the art wireless energy-harvesting sensors. The remodeled SHM algorithm benefits from the sensor nodes' ability to support automated triggering and data pre-processing. The Random Decrement technique was included in the algorithm as a pre-processing tool to simultaneously reduce noise and amount of stored and transmitted data. Simulations based on available data were used to calibrate the triggering strategy, to verify the effectiveness of the data pre-processing, and to demonstrate power consumption improvements arising from the algorithm modification.

**Keywords:** Distributed sensor network, energy efficiency, intelligent infrastructure, structural health monitoring, wireless sensor networks.

### 1. INTRODUCTION

Structural Health Monitoring (SHM) is emerging as an important element for sustainable management of infrastructural systems. Ideally, future intelligent infrastructure will be equipped with embedded monitoring networks that will complement traditional methods, based on visual inspection and modeling, for maintenance purposes, (e.g. detection of early stages of degradation that may affect structural safety), and for alarm warnings (e.g. disaster notification for earthquake, explosion, etc.). Varieties of SHM methods are currently used to detect, localize, and estimate the severity of damages based on *in-situ* measurements. The reader is referred to [1 - 5] for detailed reviews on this subject. Brownjohn *et al.* 2007 [6] focused on SHM methods for civil infrastructure and identified the incorporation of sensors at the design stage and improved accessibility to the recorded data as necessary further developments of modern SHM systems.

Traditional sensor systems consist of conventional hardwired piezoelectric accelerometer networks, which have drawbacks given by the high cost of installation and maintenance, as the accessibility to the wires generally interferes with the normal operation of the structure. In the last two decades, the development of SHM approaches has been closely coupled with the evolution, miniaturization and cost reductions of digital computing hardware. Wireless Sensor Networks (WSN) are complex systems made up of a large number of electronic devices (*i.e.* sensor nodes) and constitute a promising new technology for sensing applications. Sensor nodes include a low power computational unit (*i.e.* a microcontroller or a Field-Programmable Gate Array), one or more sensors, a radio, and a power unit, which is typically a battery that may be powered by an energy harvesting module. Current research in the field of WSN for SHM purposes focuses on the investigation of data acquisition and aggregation, signal analysis, and data reduction strategies

\* Address correspondence to this author at the Department of Civil Engineering, California State Polytechnic University, Pomona, 3801 West Temple Avenue, Pomona, California, 91768 USA; Tel: +1(909) 979-5586; Fax: +1(909) 869-4342; E-mail: [glomiento@cpp.edu](mailto:glomiento@cpp.edu)

[7 - 10] aimed at reducing power consumption while still collecting high quality data for accurate offline analysis. Compared with previous studies, which focus specifically on the deployment of WSN architecture for reliable data streaming or on the SHM algorithm capability based on predetermined data quality, the approach presented in this study presents novel characteristics as it involves simultaneous adaptation of the algorithm to the WSN features and viceversa. An existing vibration based SHM algorithm [11, 12], which is currently in use on a suspension bridge instrumented with wired piezoelectric accelerometers, has been modified to include event-based triggering and pre-processing at the sensor level. The combination of these two features is aimed at reducing the amount of data transmitted by the sensors while maintaining a sufficient data quality required by the SHM algorithm. The data compaction is crucial for the reduction of the power consumption, which constrains the design of the energy harvesting module. Environmental acceleration data from the current sensor network were used as testbed data to perform a power consumption assessment of the WSN and to validate the remodeled SHM algorithm capabilities.

## 2. TESTBED DATA

Environmental accelerations recorded on the Vincent Thomas Bridge in San Pedro, California Fig. (1) were used as testbed data for the design and calibration of the new WSN system. Completed in 1964, the Vincent Thomas Bridge is a cable-suspension bridge, consisting of a main span of approximately 457 m, two suspended side spans of 154 m each, and a ten-span approach of approximately 545 m length on either end.



**Fig. (1).** Vincent Thomas Bridge overall view.

The bridge is currently subjected to a long term SHM program to monitor its performance over time. Data collection is provided by an accelerometric sensor network composed by 26 accelerometers and managed by the State of California Department of Conservation (CDC) Office of Strong Motion Studies, through the California Strong Motion Instrumentation Program (CSMIP). As shown in Fig. (2), the network consists of 16 accelerometers distributed onto the superstructure, and 10 accelerometers placed at the foundation level. A total of 11 sets of ambient-vibration acceleration records, collected from 2006 to 2011 (see Table 1), were used to calibrate and validate the effectiveness of the triggering and pre-processing process, in terms of quality of modal identification.

**Table 1.** Acceleration data set.

No	Year	Date	Hour	Length (sec)
1	2006	7 Dec	14:57:40.0	67.0
2	2007	11 July	08:58:27.0	58.0
3	2007	7 August	09:31:37.0	61.0
4	2011	7 June	09:59:38.0	54.0
5	2011	7 June	21:59:39.0	55.0
6	2011	14 June	09:59:38.0	54.0
7	2011	14 June	21:59:39.0	54.0
8	2011	21 June	09:59:38.0	54.0
9	2011	21 June	21:59:39.0	54.0
10	2011	28 June	09:59:38.0	54.0
11	2011	28 June	21:59:39.0	54.0

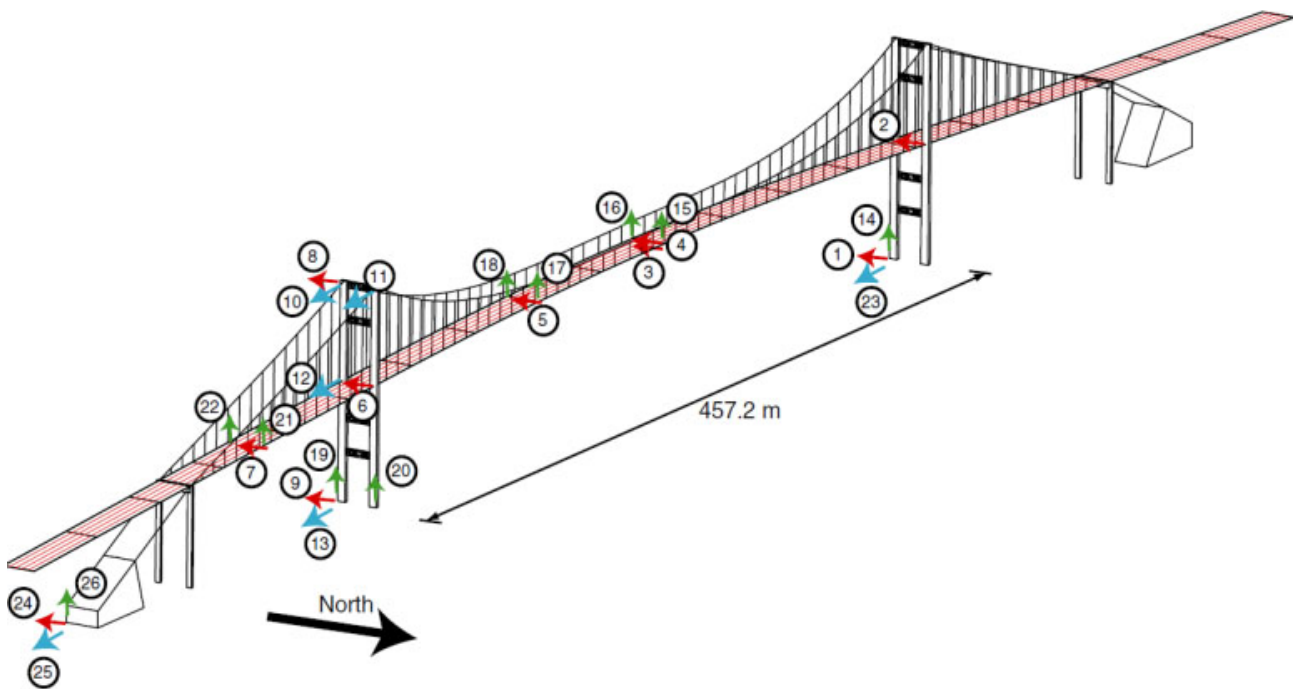


**Fig. (2).** Vincent Thomas Bridge sensor location.

### 3. STRUCTURAL HEALTH MONITORING SYSTEM

The existing SHM algorithm uses acceleration records from a dispersed set of sensors to obtain information about the condition of the entire structure. The core of the algorithm compares the modal energy of the structure in the undamaged and damaged state, as indicative of the degradation experienced on local portions of the overall structural assembly. A structural identification procedure is required in order to evaluate vibration mode characteristics of the structure from acceleration records. The main steps of the SHM algorithm are synthesized in Fig. (3). Further details about the algorithm are given in [11, 12].

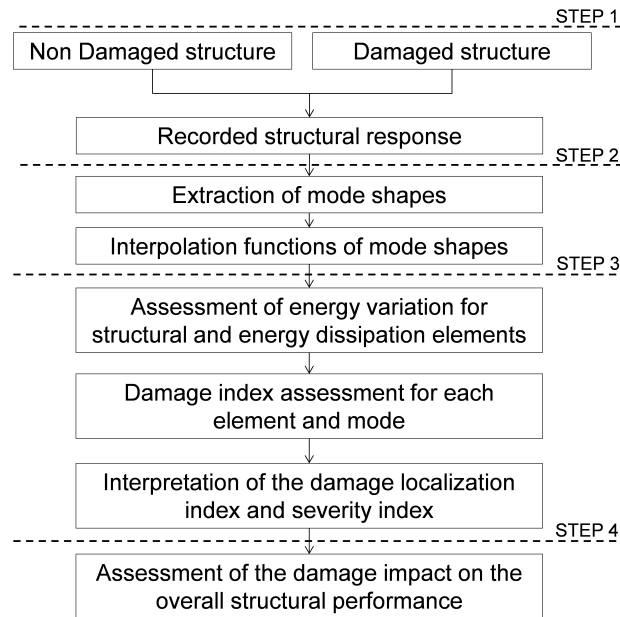


Fig. (3). SHM algorithm flow-chart.

Computation and transmission capabilities of the new wireless sensor nodes are used to guarantee high quality data for the identification of the bridge mode shapes (Step 2), while reducing the sensor power consumption. In details, the Wireless communication of the network nodes is used to perform correlation analysis of the structural vibrations, in order to trigger data recording and storing when significant vibration events are recognized. Furthermore, a data pre-processing through the Random Decrement (RD) technique [13] has been used to improve the quality of the data recorded during the triggering events. The RD technique provides also data compaction and consequent reduction of the energy required for their transmission, which is the main source of the sensor power consumption.

#### 4. TRIGGERING AND PRE-PROCESSING

The event-based strategy is a natural way to acquire data in intelligent sensors. If the trigger-event is associated with intense vibration of the structure, the event-driven sampling reduces the amount of stored and processed data without deterioration of the signal tracking performance because the data analysis occurs only when it is required. The condensation of raw data, in order to extract meaningful information, is made possible by the onboard computational capability of smart sensors.

##### 4.1. Event-Based Triggering Strategy

The monitoring system network is designed to have trigger and non-trigger sensor nodes. Trigger nodes are a small subset of the network nodes that detect an event if a threshold value is exceeded. Once an event has been detected a message is sent to the non-trigger nodes that start data storage for the pre-processing. Among the available sensors, for which acceleration histories are available, 6 sensors (#15, 16, 17, 18, 21, and 22) on the deck, and 3 sensors (#10, 11, and 12) on the towers are chosen as trigger sensors.

In order to guarantee the data quality required for the structural identification of the vibration modes, an event based-strategy is proposed to recognize acceleration records associated to vibration patterns of the whole structure. Outlier values, *i.e.* unusual observations unlikely belonging to the pattern or variability produced by other observations, should be excluded as unrelated to the dynamic performance of the bridge. Rather than choosing an absolute value of the instant acceleration as a threshold parameter, the Root Mean Square (RMS) of the acceleration on a fixed-length window is used as a robust measure of the amplitude of the signal. Acceleration data collected from the trigger sensors are then associated to a multivariate process, and the Mahalanobis distance [14] is used to assess the RMS Window Length (WL) in order to reduce the number of outlier values. The adopted method for the outlier detection was implemented by the following 4 steps:

**Step 1.** Evaluation of the Mahalanobis distance based on the available data from the data set of Table 1, combined in a single signal. The Mahalanobis distance was evaluated for single values measured by the accelerometers and for RMS acceleration values with WL from 0.1 to 60 sec. Given a number  $p$  of sensors installed on the bridge, the squared Mahalanobis distance is obtained as:

$$D^2(\mathbf{x}) = (\mathbf{x} - \boldsymbol{\mu})^T \mathbf{S}^{-1} (\mathbf{x} - \boldsymbol{\mu}) \tag{1}$$

where  $\mathbf{x}$  is the observation multivariate vector  $\mathbf{x} = (x_1, x_2, x_n)$  from a group of values with mean  $\boldsymbol{\mu} = (\mu_1, \mu_2, \mu_n)$  and covariance matrix  $\mathbf{S}$ .

**Step 2.** Plot of the squared Mahalanobis distances  $D^2$  against the quantile of the chi-square distribution  $X_p^2$ . In this chi-square plot introduced by [15], outliers are identified as departing points from a straight line representing the  $X_p^2$  distribution.

**Step 3.** Evaluation of the 95% simultaneous confidence band for the residuals between the quantile of the Mahalanobis distance and the  $X_p^2$  distribution by means of the Kolmogorov-Smirnov two-sample distribution.

**Step 4.** Identification of the outlier values (points exceeding the confidence band), and evaluation of the Outlier to Measured data Ratio (OMR) computed as the number of outliers divided by the number of available data.

Chi-square plots for single acceleration values, WL=1 sec and WL=60 sec are reported in Fig. (4a-f) for bridge deck and towers, respectively. The 95% simultaneous confidence intervals were added to the plots as dotted lines.

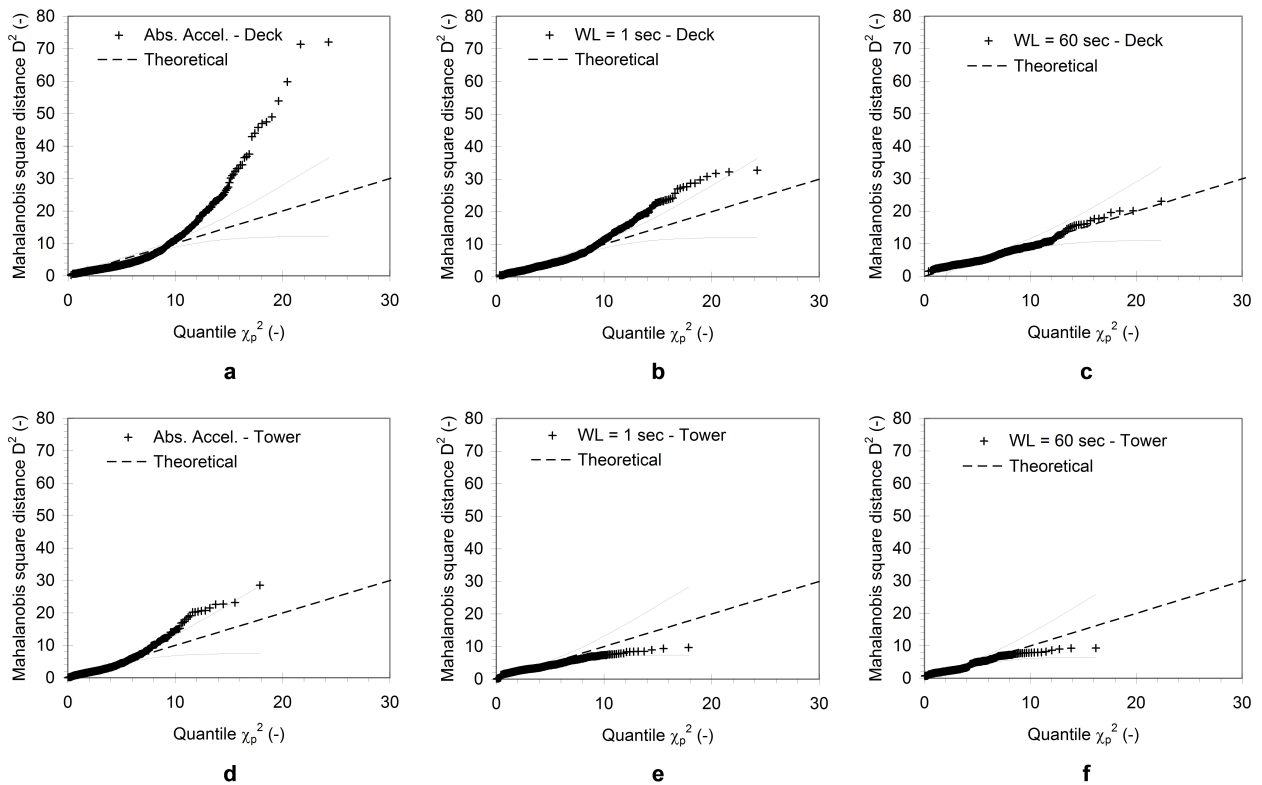


**Fig. (4).** Mahalanobis distance vs. quantile chi square distribution of the acceleration data with 95% simultaneous confidence band, for the deck: (a) absolute punctual acceleration (Outlier to Measured data Ratio, OMR = 81.1%); (b) Window Length (WL) = 1 sec (OMR = 74.4%); (c) WL = 60 sec (OMR = 0.0%); for the towers: (d) absolute punctual acceleration (OMR = 43.0%); (e) WL = 1 sec (OMR = 58.3%); (f) WL = 60 sec (OMR = 22.7%).

The RMS with WL=60 sec (Fig. 4f) showed the minimum deviation from the theoretical chi-square distribution,

represented as a dashed line. For this WL, the minimum values of OMR (0.0% and 22.7% for the deck and the towers, respectively) were identified. Based on these results the RMS of the acceleration data on a 60 sec window was chosen as triggering parameter. It should be noted that the OMR=22.7% value for the towers is due to points exceeding the confidence band for quintile values not greater than 1.5. These points are associated with low acceleration measures, very frequently exceeded and inadequate as threshold values for the triggering check.

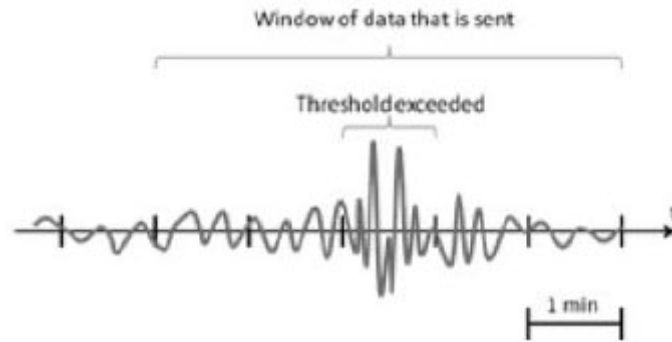


Fig. (5). Data-window sent in a triggering event.

In order to implement the triggering strategy in the WSN, sensor nodes record data continuously. The accelerometer sample is stored on the node memory and used to update the RMS of the acceleration along the three axes during the last 60 sec window. An online algorithm [16] is used to reduce the number of interrogations of the memory and speed up the computation of the RMS acceleration. An event is detected when the RMS acceleration over the previous 60 sec window is above the threshold. Once the event has been detected, data are collected on a 5 minutes window which includes three minutes of pre-event and 2 minutes of past-event as shown in Fig. (5).

4.2. Pre-Processing Data Condensation

The accuracy and reliability of vibration based SHM techniques in actual field applications may suffer from the influence of environmental and service conditions on the dynamic response of the structure. Changes in the modal signature caused by structural deterioration can be masked under these effects [17 - 19]. The Random Decrement (RD) technique [13] can be used to reduce noise of experimentally measured structural responses. More details and applications of the RD technique can be found in [20]. Due to its very simple estimation algorithm [21] with respect to other data compaction methods, the RD technique can efficiently be implemented on low power, low cost microcontrollers, resulting in a lower sensor nodes' energy consumption.

According to the RD technique, the response of a system to random input loads, at time instant,  $t$ , is assumed as the summation of the response to an initial displacement, the response to an initial velocity, and the response to the random input loads between the initial state and the time instant  $t$ . By averaging a large number of time segments of the response with the same initial condition, the random part of the response vanishes, while the response of the system to the initial conditions remains. Therefore, measured acceleration time histories can be transformed into free vibrations by the RD method with a significant reduction of data. The data condensation provided by the RD method is expressed by the ratio  $n/N$ , where  $n$  and  $N$  are the size of the RD time segment and the measured acceleration vector, respectively.

Two RD methods, for the estimates of auto- and cross-correlation functions [22] were investigated in order to assess the quality of the structural identification procedure and set appropriate parameters for the initial conditions and the time segment length. For the time series  $y(t)$  and  $z(t)$ , the estimates of the auto- and cross-correlation functions are obtained as the empirical mean:

$$D_{yy}(\tau) = \frac{1}{K} \sum_{i=1}^K y(\tau + t_i) | C_{y(t_i)} \tag{2}$$

$$D_{zy}(\tau) = \frac{1}{K} \sum_{i=1}^K z(\tau + t_i) | C_{y(t_i)} \tag{3}$$

where  $K$  is the number of time segments fulfilling the threshold condition  $C_{y(t_i)}$ . Several threshold conditions can be formulated which only pick out either the correlation functions or the derivative of the correlation functions [23]. In this work, the upcrossing condition  $C_{y(t_i)} : (y_i > th)$  is considered and the threshold level  $Th$  is expressed in terms of standard deviation  $\sigma$  of the  $y(t)$ . The RD techniques for the auto- and cross-correlation functions belong, respectively, to the two broad categories of decentralized data aggregation approaches: (a) independent processing (each node processes sensor data independently), and (b) coordinated processing (sensor nodes collaborate to process sensor data by sharing information). The choice between the two methods derives from both the quality assessment of the structural identification and the efficiency evaluation in terms of power consumption.

The quality assessment of the RD techniques for structural identification is based on the Modal Assurance Criteria, [24] as shown in the following steps. With this aim, first the RD auto- and cross-correlation functions are evaluated from the data for a number of upcrossing thresholds  $Th = [1 \ 1.25 \ 1.5 \ 1.75 \ 2]\sigma$  and sizes of the RD window  $n = [1000 \ 2000 \ 3000 \ 4000 \ 5000]$ , corresponding to time segments of  $[10 \ 20 \ 30 \ 40 \ 50]$  sec. Then, the modal characteristics (frequency, damping and shape) are identified by means of the covariance-driven stochastic subspace identification method (SSI-Cov) [25]. A high system order (200) was chosen in order to reduce the bias on the estimates and allow capturing all relevant characteristics of the structure despite measurement noise. Pole values were extracted at different orders and following values are used as assurance criteria: 1% for frequency stability, 5% for damping stability, and 2% for eigenvector stability. Finally, a modal quality index was defined to compare the quality of the system identification of all the analyzed cases. The index is defined as the ratio between the number of stable poles and model order for the first three modes.

Statistics of the modal quality index vs. the window size  $n$  are presented in Fig. (6a and b), for the application of the RD technique with auto and cross correlation function, respectively. The full length value means that data were used without pre-processing via RD technique. The bottom and top of the box are the 25<sup>th</sup> and 75<sup>th</sup> percentile, the dashed line joins 50<sup>th</sup> percentile (median) values, and the ends of the whiskers represent the minimum and maximum of all the data. The modal quality index shows peak values for a window size  $n=2000$ , for both the application with auto and cross correlation functions. The highest quality values are obtained with the cross correlation functions. Peak values of the modal quality index are higher than values obtained without using the RD technique. From Fig. (6a and b), the MAC for a window size  $n=2000$  is even higher than the value obtained for full length records. This means that despite the data compaction, the combination of the triggering strategy and the RD pre-processing technique provides an improvement in the identification of the modal shapes used in the SHM algorithm.

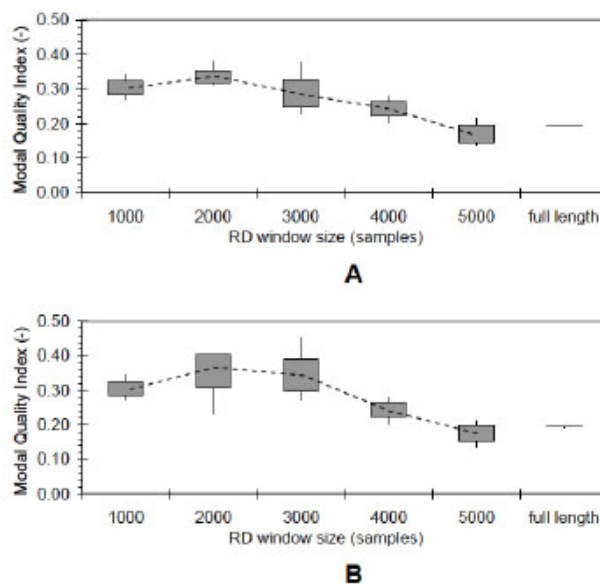


Fig. (6). Modal quality index vs. RD-window size for (A) auto correlation and (B) cross correlation functions.

In Fig. (7a and b), statistics of the modal quality index are reported vs. the threshold  $Th$  for the auto and cross correlation functions, respectively. Even if a trend of the modal quality index with the threshold level  $Th$  is not visible,

the lowest dispersion of the values, indicated by the width of the boxes, was found for  $Th = 1.75\sigma$  and  $1.5\sigma$  for the auto and cross correlation functions, respectively. This quality assessment suggests that the most beneficial application of the RD technique for the examined case consists in the use of cross correlation functions with threshold  $Th=1.5\sigma$ .

## 5. WSN ARCHITECTURE

The implementation of the triggering and the pre-processing techniques requires a wireless network composed of multiple nodes and a base station. A node consists of a mote and a sensor board. The node measures vibrations, continuously samples and locally stores data from an embedded accelerometer. Each node needs to be designed to have enough memory and computational capabilities to perform local data collection and pre-processing. The sensors are required to provide local distributed data analyses, which are more power efficient than streaming all the samples to a backend server.

A detailed design of the WSN architecture is needed to allow the assessment of the power consumption. The software architecture of the nodes proposed for the Vincent Thomas Bridge application uses some components integrated into the Zigbee based wireless sensor node to satisfy the requirements discussed above. In Fig. (8) the architecture of the proposed wireless sensor node for the VTB Structural Health Monitoring is shown. The specific features proposed for the nodes are presented in the following sub-sections.

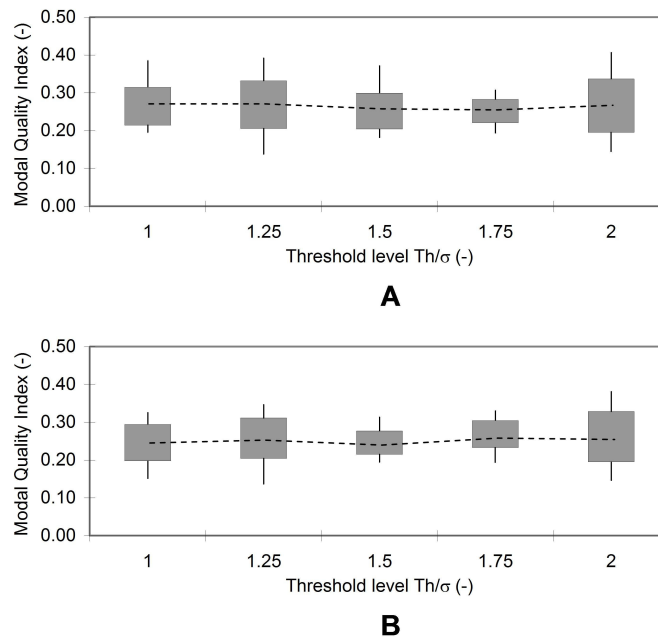


Fig. (7). Modal quality index vs. threshold level  $Th$  for (A) auto correlation and (B) cross correlation functions.

**Microcontroller.** In order to limit the power consumption, a low power Micro Control Unit (MCU) is required as core of the nodes. Specifically, the proposed sensor node includes a low power 32 bit MCU AT32UC3A0512 from Atmel [26] which is able to operate at up to 66MHz. The MCU features 512KBytes of program memory, 64 KBytes of built in RAM and a number of peripheral (SPI, UART, Timers *etc.*) and external interrupts that are used to communicate with the other components of the node.

**Digital accelerometer.** Because of structural interest in local modes of vibration, a sampling rate of 100 Hz is chosen as target rate. With this aim, the node embeds the ultra low-power, high performance three axes linear digital accelerometer LIS331DLH from ST Microelectronics [27]. The accelerometer is able to sample at up to 1kHz acceleration in the range of  $\pm 2g$  with 1mg sensitivity. Each output sample is 12 bit long, so it must be stored in 2 bytes of memory. Storing the data from all three axes sampled at 100Hz requires 600Bytes/s. For this reason the 2MBytes external low power RAM FM25H20 from RAMTRON [28] is added to provide enough memory to record up to almost 1 hour of data.

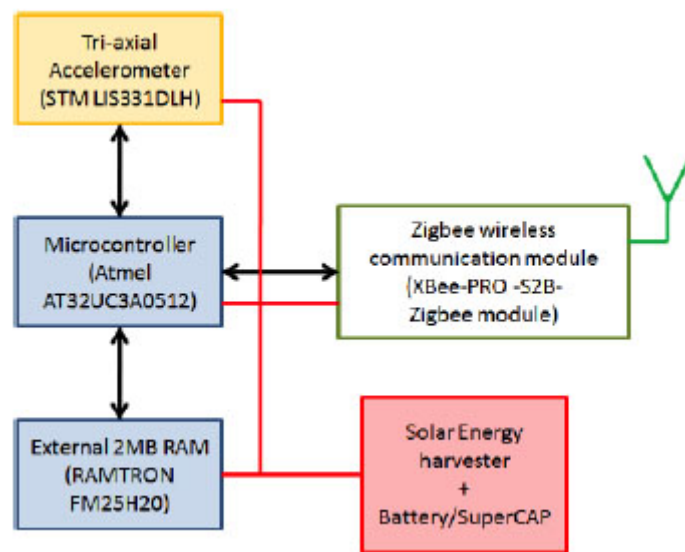


Fig. (8). Node architecture.

**Wireless communication** Wireless communication of the network nodes is required to synchronize and correlate data collected by the WSN. The wireless communication is entirely handled by the external Zigbee module XBee-PRO-S2B from Digi International [29, 30]. According to the Zigbee protocol specification, the network coordinator (the central server) periodically sends beacon messages used to synchronize the network nodes and assigns Guaranteed Time Slots (GTS) to specific nodes to quickly communicate the data collected and processed on the sensors. The initial Contention Access Period (CAP) is used for asynchronous trig messages and to communicate the position of the windows of interest in the cross correlation based algorithm.

**Network topology** Due to the great length of the main span, the Vincent Thomas Bridge installation requires a secure multihop network. The design module is able to communicate at up to 3200m in open air and set up a secure multihop wireless network. Given the available extended range, the nodes of the network are organized in a star topology where each node is a low power, sleep, end device and the central server acts as the coordinator and manages all the node to node communication. The use of a star topology and the beacon reduces the complexity and power consumption associated to the wireless communication of the network nodes. In fact, the nodes should not keep routing table of their neighbor nor synchronize with multiple sensor nodes. Furthermore there is no need to execute complex time synchronization techniques to compensate for clock drift on different devices. Table 2 synthesizes the current consumption of the node when operating in different states, and shows that wireless transmitting is the main source of power consumption for a node. However, thanks to the availability of a MCU, sensor nodes can perform local data analysis to reduce the amount of samples sent through the wireless radio.

Table 2. Power consumption of the sensor node for Structural Health Monitoring.

Operating State	Current Consumption (mA)
Sleep	4.007
Active	38.015
Transmitting	238.011
Receiving	80.011

The energy assessment of the trigger and non trigger sensor of the WSN has been performed through estimate of the sensor node power consumption as it implements the proposed technique and the energy-performance trade off for different system parameters.

**Power supply.** A solar energy harvesting module is proposed to power each network node. As the node need to be operational even in adverse conditions, a supercapacitor is proposed to secure continuous source of power. The supercapacitor is chosen in place of batteries due to its longer lifetime (10+ years compared to 5-6 year for li-ion

batteries). The size of the solar panel and the supercapacitor depends on the node power consumption and are discussed in the following sections. The local event detection and data pre-processing reduce the power consumption of the nodes and allow limiting size and cost of the solar harvester. For the choice of the solar panel and supercapacitor, two parameters should be considered: the total amount of energy needed to sustain the node operation through the 24 hours, and the total amount of energy that is used during night time. The former is used to select the solar panel size, given the location and the node exposure to direct sunlight. The latter is used to select the supercapacitor size able to sustain the node operation during night time.

The choice of the solar panel size depends on the specific location where the node is placed. For example, during spring in Southern California, the average harvested energy per day over 10 days of measurement of a 25cm<sup>2</sup> photovoltaic module is 16542J [9]. The conditions over the 10 days varied from sunny to cloudy to rainy and thus well represent the range of possible weather patterns.

Table 3 presents the maximum total energy consumption in Joule for one hour of operation for different triggering and data condensation strategies ( $Th=1.5\sigma$ ; RD window size = 2000). Six triggering strategies were simulated, in terms of average daily rate  $\lambda$ . Two additional scenarios without triggering strategies were considered, with data collected every hour and every 10 minutes. Energy consumption values were evaluated in case of data compaction with auto and cross correlation functions, as well as in case of no compaction. Results are reported for trigger and non trigger nodes.

For the two extreme cases of  $\lambda=0.2$  and measurements every 10 minutes, in order to sustain the operation of the triggering node with data-compaction during 10h night time, small-size commercial supercapacitors of 60F@5V and 90F@5V can be used, respectively.

**Table 3. Energy to sustain 1h of operation (Joule) for nodes implementing different triggering and data-condensation strategies.**

Node	Pre-processing	$\lambda=0.2$	$\lambda=0.5$	$\lambda=1$	$\lambda=2$	$\lambda=5$	$\lambda=10$	Every hour	Every 10 min
Trigger	Auto Correlation	73.5	74.0	74.3	75.1	76.2	78.5	78.6	110.1
	Cross Correlation	73.7	74.4	74.7	75.6	76.9	79.8	79.8	117.8
	No Condensation	78.8	78.8	82.5	85.0	95.0	107.5	101.3	251.2
Non trigger	Auto Correlation	60.7	61.0	61.1	61.4	61.9	62.9	62.9	76.2
	Cross Correlation	61.1	61.5	61.8	62.3	63.2	65.0	65.0	89.2
	No Condensation	66.6	66.6	70.3	72.8	82.9	95.4	89.2	239.8

## 6. POWER CONSUMPTION ASSESSMENT

The triggering and the preprocessing algorithm has been implemented and simulated through the IDE AvrStudio 6 for Atmel microcontroller. The results presented in [31, 32] have been used to model the characteristics of the Zigbee, IEEE 802.15.4 wireless transceiver. The time needed to execute the operations required by the triggering and the pre-processing technique and to communicate the data to the central server has been evaluated. A simulator was developed to estimate the nodes current consumption, by keeping track of the node operating states through the day, and computing the average current consumption over each day of simulation. Statistics of current consumption of the node were obtained from a Monte Carlo analysis simulating the network operation over 100 consecutive days. The current consumption of the sensor nodes depends on the threshold level  $Th$  and the window size  $n$  of the RD technique, as well as on the number of events detected by the trigger nodes. With an average daily rate of exceedance  $\lambda$ , the threshold of the triggering strategy determines the number of detected events. Several values of  $Th$ ,  $n$  and  $\lambda$ , were chosen to represent different triggering and pre-processing strategies, and for each parameter choice 100 simulations were performed. The number of events detected every day was modeled by a Poisson distribution with  $\lambda=[0.5, 1, 2, 5, 10]$ . Two additional scenarios with an event every hour and every 10 minutes have been considered. Events were considered generated at random time during the day with uniform probability over the 24hours, without overlaps. For each scenario 5 levels of threshold  $Th = [1, 1.25, 1.5, 1.75, 2] \sigma$ , and 6 sizes of the RD window  $n = [1000, 2000, 3000, 4000, 5000, 6000]$  were considered. A binomial distribution, with probability of success given by the probability of exceeding the threshold  $Th$ , was used to determine the number of RD windows in each event. For a normal distribution of acceleration read-outs and a threshold  $Th$  defined in terms of standard deviation  $\sigma$  of the data points, the probability of success is given by the *erf* function.

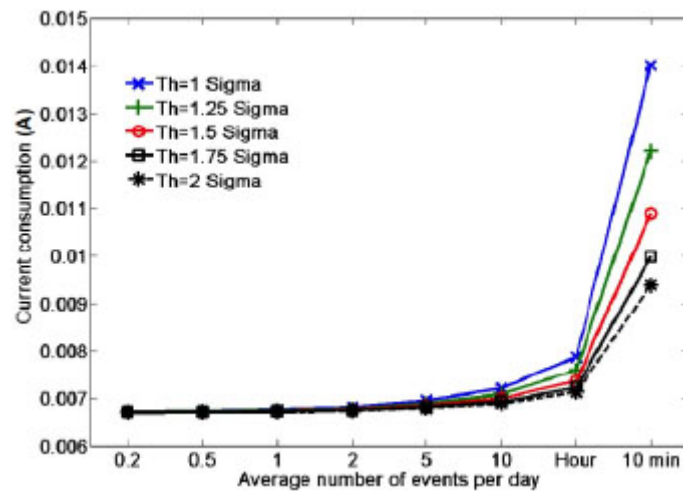


**Fig. (9).** Average node current consumption of a trigger node implementing the cross correlation technique vs. average number of events per day  $\lambda$ , for multiple thresholds  $Th$  and RD window size  $n = 2000$ .

In Fig. (9), the current consumption of a trigger node vs. the average number of events per day  $\lambda$  is represented to depict the effects of different triggering strategies. The plot refers to a node implementing the cross correlation RD technique with different values of threshold  $Th$  and  $n = 2000$  samples. As expected, the nodes current consumption increases as  $\lambda$  raises since a larger number of events per day are handled. On the other hand, the current consumption decreases with the increase of  $Th$  since for each event a smaller number of RD windows should be averaged. Note that the node current consumption never drops below 6.718mA which represents the current consumption of a node that does not detect any event for the entire day. Non trigger nodes and nodes implementing the auto correlation RD technique present similar trends.

The effects of the data compaction algorithm in terms of power consumption are presented in Table 4, for trigger and non trigger nodes. Values refer to nodes transmitting data without condensation, as well as with condensation through the auto and cross correlation RD technique, for two scenarios ( $\lambda=5$  and “every 10 minutes”), with  $Th=1.5\sigma$ , and RD window size=2000 samples.

**Table 4. Nodes current consumption (mA).**

Node	$\lambda=5$			Every 10 minutes		
	Auto Correlation	Cross Correlation	No Condensation	Auto Correlation	Cross Correlation	No Condensation
Trigger	7.05±0.05	7.12±0.06	8.80±0.25	8.26±0.01	10.90±0.01	23.25±0
Non Trigger	5.73±0.02	5.85±0.04	7.67±0.26	7.06±0.01	10.19±0.01	22.20±0

Table 4 shows that nodes implementing the cross or auto correlation RD technique present similar current consumption. Considering the scenario  $\lambda=5$ , nodes transmitting data with no condensation have a current consumption about 25-30% higher than the consumption of nodes implementing the data condensation. The benefits of the data condensation are even more evident for a greater number of events detected per day. If events are detected every 10 minutes, the current consumption with no condensation becomes even 110% higher than the consumption with data condensation.

The impact of the RD window size on the node current consumption is reported in Fig. (10). This plot shows the current consumption vs. the RD window size. A consistent reduction of current consumption is achieved by reducing the RD window size. As previously discussed, the window size is also the parameter that mainly affects the quality of the structural identification required by the SHM algorithm.

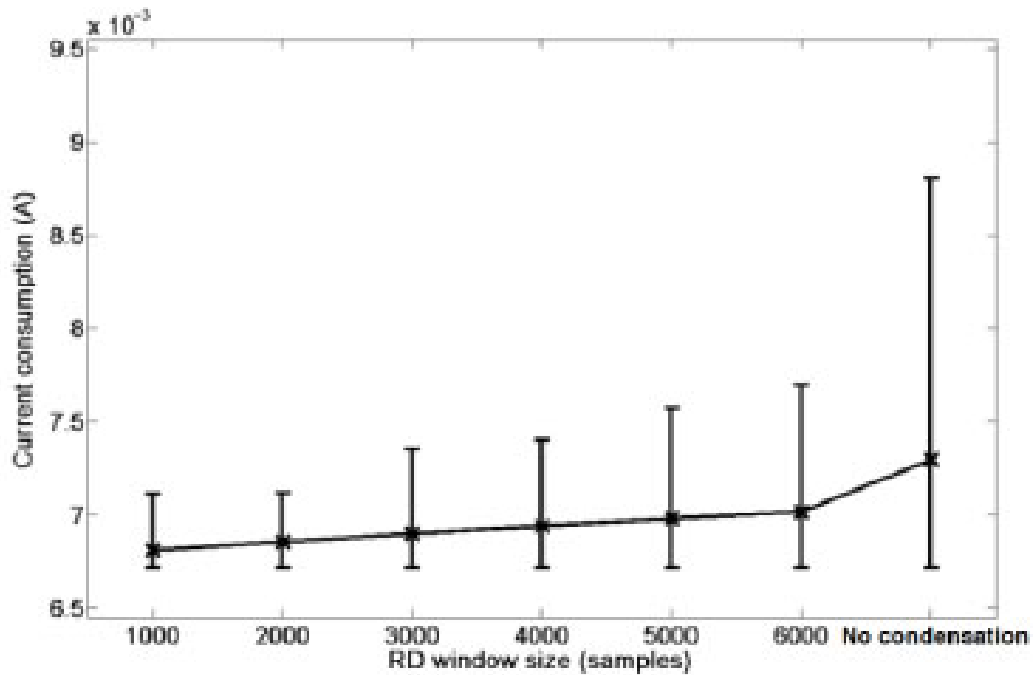


Fig. (10). Average, max and min node current consumption of a trigger node implementing the cross correlation algorithm vs. the RD window size ( $Th=1.5\sigma$ ,  $\lambda = 5$  samples).

In Fig. (11), the modal quality index values of Fig. (5b) are combined with the current consumption values of Fig. (10). The resulting plot shows the variation of the modal quality index vs. the current consumption.

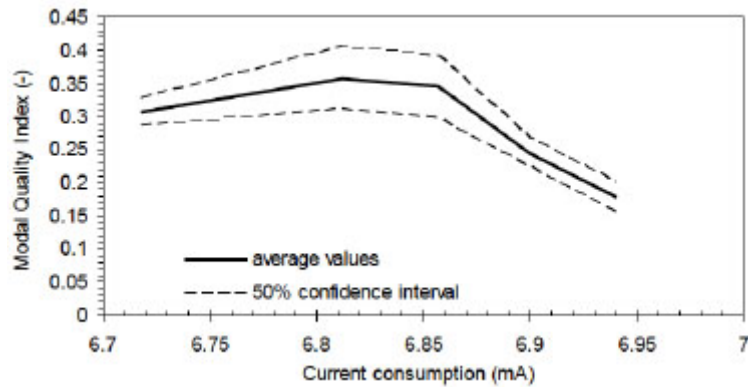


Fig. (11). Modal quality index vs. daily current consumption ( $Th=1.5\sigma$ ,  $\lambda = 5$  samples).

The modal quality index increases until the current consumption value of 6.812 mA is reached. This value corresponds with the implementation at the node level of the pre-processing RD technique with cross correlation functions on a window of 2000 acceleration samples. Values of current consumption greater than 6.812 mA are associated with an RD windows size  $n > 2000$ . As shown before, rather than increasing the modal quality index, any increment of size over 2000 samples generates, for the considered case study, a reduction of the quality of the modes.

**CONCLUSION**

An SHM algorithm able to detect damages on bridges equipped with wired sensors has been improved to benefit from computational capabilities of innovative WSN. A triggering strategy and a data-condensation technique have been designed to be implemented in the sensor nodes. The triggering strategy allows recognizing significant vibration events and excluding outlier values unrelated to the dynamic performance of the bridge. Despite the reduction of the amount of data, the data compaction performed by applying the RD technique on trigger-events proved able to increase the quality

of the modal identification from recorded data.

The triggering strategy and the data-condensation are also beneficial in reducing power consumption of the WSN. The implementation of these features on the sensor nodes allowed designing an energy efficient, solar powered sensor network. The size and cost of the proposed sensor nodes is limited and dominated by the solar panel and the supercapacitors. This motivates the use of the proposed combination of triggering and pre-processing techniques to reduce the nodes energy consumption. In fact, the MCU, the transceiver, the RAM and the accelerometer are embedded in package of few cm<sup>2</sup> (14×14mm, 24×33mm plus the antenna, 5×6mm, and 3×3mm respectively), while the size of each of the 2 supercapacitors needed to obtain the 5V to power the sensor node is 35x50mm. Based on the available data, the proposed sensor system appears as a valuable option for cost-effective monitoring of bridges.

## CONFLICT OF INTEREST

The authors confirm that this article content has no conflict of interest.

## ACKNOWLEDGEMENTS

Declared none.

## REFERENCES

- [1] S. W. Doebling, C. R. Farrar, M.B. Prime, and D.W. Shevitz, "*Damage Identification and Health Monitoring of Structural and Mechanical Systems from Changes in Their Vibration Characteristics: A Literature Review*", Los Alamos National Laboratory Report LA-13070-MS, 1996.
- [2] P.C. Chang, A. Flatau, and S.C. Liu, "Review paper: health monitoring of civil infrastructure", *Struct. Health Monit.*, vol. 2, no. 3, pp. 257-267, 2003.  
[<http://dx.doi.org/10.1177/1475921703036169>]
- [3] H. Sohn, and M. Dzwonczyk, "E.G. Straser, A.S. Kiremidjian, K.H. Law, and T. Meng, "An experimental study of temperature effect on modal parameters of the Alamosa Canyon Bridge", *Earthq. Eng. Struct. Dynam.*, vol. 28, pp. 879-897, 1999.  
[[http://dx.doi.org/10.1002/\(SICI\)1096-9845\(199908\)28:8<879::AID-EQE845>3.0.CO;2-V](http://dx.doi.org/10.1002/(SICI)1096-9845(199908)28:8<879::AID-EQE845>3.0.CO;2-V)]
- [4] C.R. Farrar, and K. Worden, "An introduction to structural health monitoring", *Philos. Trans. A. Math. Phys. Eng. Sci.*, vol. 365, no. 1851, pp. 303-315, 2007.  
[<http://dx.doi.org/10.1098/rsta.2006.1928>] [PMID: 17255041]
- [5] W. Fan, and P. Qiao, "Vibration-based damage identification methods: a review and comparative study", *Struct. Health Monit.*, vol. 10, no. 1, pp. 83-111, 2011.  
[<http://dx.doi.org/10.1177/1475921710365419>]
- [6] J.M. Brownjohn, "Structural health monitoring of civil infrastructure", *Philos. Trans. A. Math. Phys. Eng. Sci.*, vol. 365, no. 1851, pp. 589-622, 2007.  
[<http://dx.doi.org/10.1098/rsta.2006.1925>] [PMID: 17255053]
- [7] S. Kim, S. Pakzad, D. Cullert, J. Demmelt, G. Fenest, S. Glasert, and M. Turon, "Health monitoring of civil infrastructures using wireless sensor networks", In: *Proceedings of International Conferences on Information Processing in Sensor Networks*. 2007, pp. 254-263.  
[<http://dx.doi.org/10.1109/IPSNS.2007.4379685>]
- [8] C.R. Farrar, G.D. Park, W. Allen, and M.D. Todd, "Sensor network paradigms for structural health monitoring", *J. Struct. Control Health Monit.*, vol. 13, no. 1, pp. 210-225, 2006.  
[<http://dx.doi.org/10.1002/stc.125>]
- [9] A. Ravinagarajan, D. Dondi, and T.S. Rosing, "DVFS based task scheduling in a harvesting WNS for structural health monitoring", In: *Proceedings of the Conference on Design, Automation and Test in Europe*. Dresden, 2010, pp. 1518-1523.  
[<http://dx.doi.org/10.1109/DATE.2010.5457052>]
- [10] S.C. Mukhopadhyay, and I. Ihara, "Sensors and technologies for structural health monitoring: a review", *New Dev. Sensing Technol. Struct. Health Monit. Lect. Notes Electr. Eng.*, vol. 96, pp. 1-14, 2011.  
[[http://dx.doi.org/10.1007/978-3-642-21099-0\\_1](http://dx.doi.org/10.1007/978-3-642-21099-0_1)]
- [11] N. Bonessio, G. Lomiento, and G. Benzoni, "Damage identification procedure for seismically isolated bridges", *Struct. Control Health Monit.*, vol. 19, no. 5, pp. 565-578, 2012.  
[<http://dx.doi.org/10.1002/stc.448>]
- [12] G. Benzoni, N. Bonessio, and G. Lomiento, "Structural health monitoring of bridges with anti-seismic devices", In: *Proceedings of European Conference on Structural Dynamics*, 2011, pp. 4-6.
- [13] H.A. Cole, American Institute of Aeronautics and Astronautics, "On-The-Line analysis of random vibrations", In: *9<sup>th</sup> Structural Dynamics and Materials Conference*. Palm Springs: CA, USA, 1968, pp. 68-288.
- [14] I. Ben-Gal, "Outlier detection", In: Maimon O., and Rockach L., Eds., *Data Mining and Knowledge Discovery Handbook: A Complete Guide*

- for Practitioners and Researcher. Kluwer Academic Publisher, 2005.  
[[http://dx.doi.org/10.1007/0-387-25465-X\\_7](http://dx.doi.org/10.1007/0-387-25465-X_7)]
- [15] R.G. Garrett, "The chi-square plot: A tool for multivariate outlier recognition", *J. Geochem. Explor.*, vol. 32, pp. 319-341, 1989.  
[[http://dx.doi.org/10.1016/0375-6742\(89\)90071-X](http://dx.doi.org/10.1016/0375-6742(89)90071-X)]
- [16] S. Wolfram, *Sample Variance Computation*, 2012. Available from: <http://mathworld.wolfram.com/SampleVarianceComputation.html>
- [17] H. Sohn, C.R. Farrar, F.M. Hemez, J.J. Czarnecki, D.D. Shunk, D. W. Stinemas, and B.R. Nadler, "A Review of Structural Health Monitoring Literature: 1996–2001", Los Alamos National Laboratory Report, LA-13976-MS, 2001.
- [18] F.N. Catbas, and A.E. Aktan, "Condition and damage assessment: issues and some promising indices", *J. Struct. Eng.*, vol. 128, no. 8, pp. 1026-1036, 2002.  
[[http://dx.doi.org/10.1061/\(ASCE\)0733-9445\(2002\)128:8\(1026\)](http://dx.doi.org/10.1061/(ASCE)0733-9445(2002)128:8(1026))]
- [19] P.C. Chang, A. Flatau, and S.C. Liu, "Review paper: health monitoring of civil infrastructure", *Struct. Health Monit.*, vol. 2, no. 3, pp. 257-267, 2003.  
[<http://dx.doi.org/10.1177/1475921703036169>]
- [20] M. Gul, and F.N. Catbas, "Statistical pattern recognition for Structural Health Monitoring using time series modeling: Theory and experimental verifications", *Mech. Syst. Signal Process.*, vol. 23, pp. 2192-2204, 2009.  
[<http://dx.doi.org/10.1016/j.ymssp.2009.02.013>]
- [21] R. Brincker, S. Krenk, and J.L. Jensen, "Estimation of the correlation functions by the random decrement technique", In: *Proceedings of International Modal Analysis Conference and Exhibit*, 1991, pp. 14-18.
- [22] J.C. Asmussen, and R. Brincker, "Estimation of frequency response functions by random decrement", In: *Proceedings of International Modal Analysis Conference*, 1996, pp. 246-252.
- [23] J.C. Asmussen, S.R. Ibrahim, and R. Brincker, "Random decrement: identification of structures subjected to ambient excitation", In: *Proceedings of International Modal Analysis Conference*, 1998, pp. 914-921.
- [24] R.J. Allemang, "The modal assurance criterion (MAC): twenty years of use and abuse", In: *Proceedings of International Modal Analysis Conference*. 2002, pp. 397-405.
- [25] B. Peeters, "Identification and Damage Detection in Civil Engineering", Ph.D. Thesis, Department of Civil Engineering, K.U. Leuven, Belgium, 2000.
- [26] *Atmel*, 2012. Available from: <http://www.atmel.com/>
- [27] *STM*, 2012. Available from: <http://www.st.com/>
- [28] *RAMTRON*, 2012. Available from: <http://www.ramtron.com/>
- [29] *Digi International*, 2012. Available from: <http://digi.com>
- [30] *Zigbee*, "Zigbee Alliance", 2012. Available from: <http://www.zigbee.org/>
- [31] M. Kohvakka, M. Kuorilehto, M. Hännikäinen, and T.D. Hämäläinen, "Performance analysis of IEEE 802.15.4 and ZigBee for large-scale wireless sensor network applications", In: *Proceedings of the 3<sup>rd</sup> ACM International Workshop on Performance Evaluation of Wireless Adhoc, Sensor and Ubiquitous Networks, October 6*, Terromolinos, Spain, 2006.  
[<http://dx.doi.org/10.1145/1163610.1163619>]
- [32] M. Benocci, C. Tacconi, E. Farella, L. Benini, L. Chiari, and L. Vanzago, "Accelerometer-based fall detection using optimized ZigBee data streaming", *Microelectr. J.*, vol. 41, no. 11, pp. 703-710, 2010.  
[<http://dx.doi.org/10.1016/j.mejo.2010.06.014>]

Received: June 30, 2015

Revised: August 15, 2015

Accepted: August 26, 2015

© Bonessio et al; Licensee Bentham Open.

This is an open access article licensed under the terms of the Creative Commons Attribution-Non-Commercial 4.0 International Public License (CC BY-NC 4.0) (<https://creativecommons.org/licenses/by-nc/4.0/legalcode>), which permits unrestricted, non-commercial use, distribution and reproduction in any medium, provided the work is properly cited.